Acta Crystallographica Section F
Structural Biology and Crystallization Communications
ISSN 1744-3091

Expression, purification, crystallization and preliminary X-ray diffraction analysis of dihydrodipicolinate synthase from *Bacillus anthracis* in the presence of pyruvate

Jarrod E. Voss,[a,b] Stephen W. Scally,[a,b] Nicole L. Taylor,[a,b] Con Dogovski,[a,b] Malcolm R. Alderton,[c] Craig A. Hutton,[b,d] Juliet A. Gerrard,[e] Michael W. Parker,[a,b,f] Renwick C. J. Dobson[a,b]* and Matthew A. Perugini[a,b]*

[a]Department of Biochemistry and Molecular Biology, University of Melbourne, Parkville, Victoria 3010, Australia, [b]Bio21 Molecular Science and Biotechnology Institute, 30 Flemington Road, Parkville, Victoria 3010, Australia, [c]Human Protection and Performance Division, Defence Science and Technology Organization, Fishermans Bend, Victoria 3207, Australia, [d]School of Chemistry, University of Melbourne, Parkville, Victoria 3010, Australia, [e]School of Biological Sciences, University of Canterbury, Private Bag 4800, Christchurch 8020, New Zealand, and [f]St Vincents Institute of Medical Research, 9 Princes Street, Fitzroy, Victoria 3065, Australia

Correspondence e-mail: rdobson@unimelb.edu.au, perugini@unimelb.edu.au

Received 1 November 2008
Accepted 7 January 2009

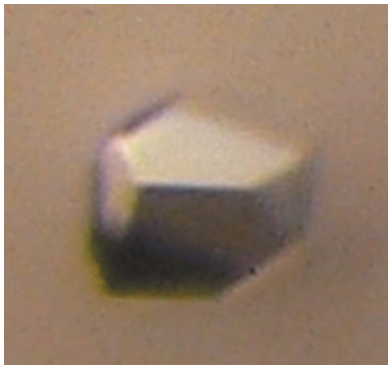

Dihydrodipicolinate synthase (DHDPS) catalyses the first committed step in the lysine-biosynthesis pathway in bacteria, plants and some fungi. In this study, the expression of DHDPS from *Bacillus anthracis* (*Ba*-DHDPS) and the purification of the recombinant enzyme in the absence and presence of the substrate pyruvate are described. It is shown that DHDPS from *B. anthracis* purified in the presence of pyruvate yields greater amounts of recombinant enzyme with more than 20-fold greater specific activity compared with the enzyme purified in the absence of substrate. It was therefore sought to crystallize *Ba*-DHDPS in the presence of the substrate. Pyruvate was soaked into crystals of *Ba*-DHDPS prepared in 0.2 *M* sodium fluoride, 20%(*w*/*v*) PEG 3350 and 0.1 *M* bis-tris propane pH 8.0. Preliminary X-ray diffraction data of the recombinant enzyme soaked with pyruvate at a resolution of 2.15 Å are presented. The pending crystal structure of the pyruvate-bound form of *Ba*-DHDPS will provide insight into the function and stability of this essential bacterial enzyme.

1. Introduction

The lysine-biosynthetic pathway in bacteria, also known as the diaminopimelate (DAP) pathway, leads to the *de novo* synthesis of lysine, which is essential for protein synthesis. Equally important is the immediate precursor to lysine, *meso*-DAP, which is a vital constituent of the bacterial cell wall, where it is incorporated into the peptidoglycan layer (Hutton *et al.*, 2007). The reaction catalyzed by DHDPS is the first committed step in this pathway and involves the condensation of pyruvate and (*S*)-aspartate semialdehyde [(*S*)-ASA] to form (4*S*)-4-hydroxy-2,3,4,5-tetrahydro-(2*S*)-dipicolinic acid (HTPA; Blickling *et al.*, 1997). The reaction proceeds *via* a ping-pong kinetic mechanism in which pyruvate binds as a Schiff base to an active-site lysine residue (Lys163 for *Bacillus anthracis* DHDPS), resulting in the formation of an imine. Tautomerization of the Schiff base to an enamine then occurs, although the exact mechanism of this step is unknown. (*S*)-ASA then reacts with this enamine and following cyclization forms the product HTPA (Blickling *et al.*, 1997).

The structure of ligand-free DHDPS has been determined for a number of species of bacteria, including *B. anthracis* (Blagova *et al.*, 2006), *Escherichia coli* (Dobson *et al.*, 2005), *Mycobacterium tuberculosis* (Kefala *et al.*, 2008), *Thermoanaerobacter tengcongensis* (Wolterink-van Loo *et al.*, 2008), *Thermotoga maritima* (Pearce *et al.*, 2006) and methicillin-resistant *Staphylococcus aureus* (MRSA; Burgess *et al.*, 2008). The structure of the enzyme bound to pyruvate has also recently been solved for DHDPS from *E. coli* (PDB code 3du0; Devenish *et al.*, 2008) and *S. aureus* (PDB code 3di1; Girish *et al.*, 2008). The enzyme usually assembles as a tetrameric protein, best described as a dimer of tight dimers, although an active dimeric form has recently been reported for DHDPS from MRSA (Burgess *et al.*, 2008). Each monomer is an $(\alpha/\beta)_8$-barrel, with the active site situated near the central cavity of the barrel. For those enzymes inhibited by lysine, two allosteric binding sites are located at the tight dimer interface, displaced from the active site (Dobson *et al.*, 2004).

DHDPS enzymes from plants (Frisch *et al.*, 1991; Dereppe *et al.*, 1992) and some Gram-negative bacteria (Laber *et al.*, 1992) are feedback-regulated by lysine acting as an allosteric modulator through partial inhibition of catalytic activity. However, allosteric regulation by lysine at biologically relevant concentrations has not been found in DHDPS enzymes from Gram-positive species (Cremer *et al.*, 1988; Burgess *et al.*, 2008) and thus the regulatory mechanism of these enzymes is not yet understood. Interestingly, recent studies show that pyruvate, the first substrate to bind to the DHDPS enzyme (Dobson *et al.*, 2004), stabilizes the oligomeric structure of DHDPS from MRSA (Burgess *et al.*, 2008). In this study, we therefore aimed to express, purify and soak crystals of recombinant *B. anthracis* DHDPS (*Ba*-DHDPS) with the substrate pyruvate. We show that when purified in buffers containing pyruvate the recombinant *Ba*-DHDPS enzyme has a significantly higher specific activity than *Ba*-DHDPS purified in the absence of pyruvate. Therefore, it is of interest to examine the crystal structure of the enzyme soaked with this substrate.

2. Methods and materials

2.1. Cloning and expression of *Ba*-DHDPS

The *dapA* gene encoding *Ba*-DHDPS was amplified from genomic DNA extracted from the *B. anthracis* Sterne strain using the primers 5′-TCAGCAGATAGTCATACGAC-3′ and 5′-TGAAGAACTGGTTAATGATC-3′. The PCR product was then ligated into pCR-BluntII-TOPO and transformed into *E. coli* One Shot TOP10. The *dapA* insert was then amplified from pCR-BluntII-TOPO/*dapA* using the primers 5′-CATATGATAGATTTTGGGACAAT-3′ and 5′-GATCCTTAACGAGGGATAGATTGCA-3′, which contain *Nde*I and *Bam*HI restriction-endonuclease sites, respectively. The product, which now contains *Nde*I and *Bam*HI restriction-endonuclease sites, was ligated into pCR-BluntII-TOPO and transformed into *E. coli* One Shot TOP10, which enables efficient ligation into an expression vector. The resulting plasmid and pET-11a were digested using the restriction enzymes *Nde*I and *Bam*HI and subsequently electrophoresed on a 1%(*w*/*v*) agarose gel. *Dap*A and linearized pET-11a were excised from the gel and purified before being ligated with T4 DNA ligase and transformed into *E. coli* BL21(DE3).

A 4 l expression of *E. coli* BL21-DE3(pET-11a/*dapA*) took place in Luria Broth containing 100 µg ml^{-1} ampicillin at 310 K with shaking until an OD_{600} of 0.6 was achieved. Expression of recombinant *Ba*-DHDPS was attained following the addition of IPTG to a final concentration of 1.0 m*M* and subsequent incubation at 310 K for a further 3 h. Cells were then pelleted at 10 000*g* for 15 min at 277 K, resuspended in 20 m*M* Tris–HCl pH 8.0 and frozen at 253 K until needed.

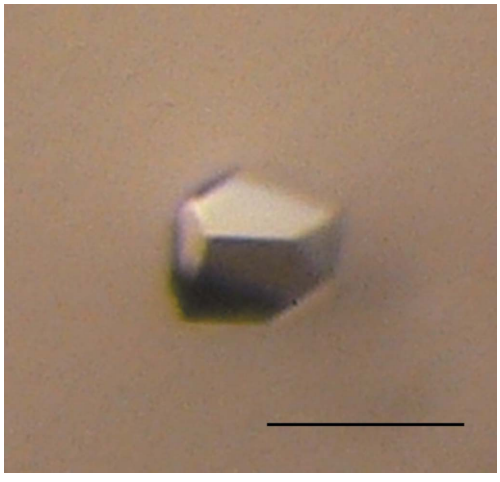

Figure 1
Ba-DHDPS crystal. The bar indicates 50 µm.

2.2. Purification of *Ba*-DHDPS

Ba-DHDPS was purified using two approaches: in the absence of pyruvate (preparation 1) and in the presence of pyruvate (preparation 2). Cells were thawed on ice for 2 h and lysed by sonication with an MSE Soniprep 150 sonicator at 14 µm amplitude. A cycle involving 8 min of 3 s bursts followed by 10 s rests was employed. The preparation was then centrifuged at 10 000*g* for 17 min at 277 K and the supernatant was subsequently collected and filtered through a 0.45 µm membrane. The crude extract was then injected onto a Q Sepharose column pre-equilibrated in buffer *A* (20 m*M* Tris–HCl pH 8.0 for preparation 1 and 20 m*M* Tris–HCl, 5 m*M* pyruvate pH 8.0 for preparation 2) at 277 K. The column was then washed with buffer *A* until a stable baseline was reached. Elution of bound protein was performed over five column volumes using a 0–1.0 *M* NaCl gradient in buffer *A* and 10 ml fractions were collected. DHDPS-containing fractions were pooled and ammonium sulfate was added to a final concentration of 500 m*M*. Pooled fractions were injected onto a Phenyl Sepharose column pre-equilibrated in buffer *B* (20 m*M* Tris–HCl, 500 m*M* ammonium sulfate pH 8.0 for preparation 1 and 20 m*M* Tris–HCl, 500 m*M* ammonium sulfate, 5 m*M* pyruvate for preparation 2) at 277 K. The protein was eluted using a five-column-volume gradient of 500–0 m*M* ammonium sulfate with 10 ml fractions collected at 277 K. Peak fractions were pooled, separated into 1 ml aliquots, flash-frozen in liquid nitrogen and stored at 193 K. Prior to use, protein samples were thawed and loaded onto a 5 ml HiTrap Desalting column for buffer exchange into the desired buffer.

2.3. Coupled kinetics assay

Kinetic analysis of *Ba*-DHDPS was performed using a coupled assay employing *Ba*-DHDPS and *E. coli* dihydrodipicolinate reductase (DHDPR; Coulter *et al.*, 1999). DHDPR was considered to be in excess when a twofold concentration increase did not affect the initial rate. Assays were performed in triplicate in 1.5 ml reduced-volume 10 mm path-length acrylic cuvettes in 200 m*M* bis-tris propane, 150 m*M* NaCl pH 8.0 at 303 K.

2.4. Crystallization of *Ba*-DHDPS

For crystallization trials, a solution of 14 mg ml^{-1} *Ba*-DHDPS in 20 m*M* Tris–HCl pH 8.0 was prepared. Initial protein-crystallization experiments were performed at the CSIRO node of the Bio21 Collaborative Crystallization Centre (C3; http://www.csiro.au/c3/) using the PACT Suite and the JCSG+ Suite crystal screens (Qiagen) at 281 and 293 K. These initial screens were set up using the sitting-drop vapour-diffusion method with droplets consisting of 100 nl protein solution and 100 nl reservoir solution. Reagents containing a variety of polyethylene glycols as precipitants gave a number of crystal forms at 281 and 293 K. These conditions were scaled up using the hanging-drop vapour-diffusion method with drops consisting of 2 µl protein solution and 2 µl precipitant solution at 277 K. Again, a variety of crystal forms were observed from a number of different conditions. The crystals with the best morphology were soaked with 4 µl 20 m*M* pyruvate in 50% reservoir solution. The best diffracting crystal (Fig. 1) grew from a reservoir solution containing 0.2 *M*

Table 1
Comparison of specific activity and yields of *Ba*-DHDPS purified in the absence and presence of pyruvate.

Purification step	Total protein (mg)	Total activity (U†)	Specific activity (U mg^{-1})	Yield (%)
Preparation 1‡				
Crude extract	296	601	2.00	100
Q Sepharose LC	179	855	4.80	142
Phenyl Sepharose LC	142	219	1.50	36.3
Preparation 2§				
Crude extract	391	4690	12.0	100
Q Sepharose LC	255	5100	20.0	105
Phenyl Sepharose LC	141	4650	33.0	98.0

† One activity unit (U) is defined as the consumption of 1 µmol of NADPH per minute. ‡ Purified using buffers free of pyruvate. § Purified using buffers containing 5 m*M* pyruvate.

sodium fluoride, 20%(*w*/*v*) PEG 3350 and 0.1 *M* bis-tris propane pH 8.0.

2.5. Data collection and processing

For X-ray data collection, the crystal was transferred to reservoir solution containing 20%(*v*/*v*) glycerol with 20 m*M* pyruvate and directly flash-frozen in liquid nitrogen. Intensity data were collected at 110 K at the Australian Synchrotron on the 3-BM1 beamline (McPhillips *et al.*, 2002; Evans & Pettifer, 2001) using X-rays with a wavelength of 0.9536 Å. Data were collected in 0.5° steps for one 360° pass with an ADSC Q210r image-plate detector positioned 200 mm from the crystal with an exposure time of 5 s. Diffraction data sets were processed and scaled using *MOSFLM* (Leslie, 1991) and *SCALA* (Collaborative Computational Project, Number 4, 1994).

3. Results and discussion

When *Ba*-DHDPS was purified in the presence of pyruvate (preparation 2), we observed a 22-fold increase in specific activity relative to using the same approach without pyruvate in the buffers used during purification (preparation 1) (Table 1). Similarly, the yield increased from 36.3% for preparation 1 to 98.0% for preparation 2 (Table 1). This phenomenon is reproducibly observed and thus cannot be attributed to batch variation. Interestingly, primary kinetic data obtained using the coupled assay (Coulter *et al.*, 1999) revealed a nonlinear reaction profile that activated as a function of time when the recombinant enzyme was purified in the absence of pyruvate (Fig. 2). This is often attributed to a lack of coupling enzyme (DHDPR); however, in this case increasing the coupling enzyme did not change the profile. In contrast, recombinant *Ba*-DHDPS from preparation 2 purified in the presence of pyruvate displayed linear and ideal kinetic behaviour (Fig. 2). This is interesting considering that a recent study showed that pyruvate stabilizes the most active oligomeric form of DHDPS from methicillin-resistant *S. aureus* (Burgess *et al.*, 2008). Given this recent study and our results as summarized in Table 1 and Fig. 2, we therefore sought to crystallize *Ba*-DHDPS bound to the substrate pyruvate.

Ba-DHDPS in the presence of pyruvate crystallized under identical conditions to the pyruvate-unbound form of the enzyme (Blagova *et al.*, 2006). The crystal shown in Fig. 1 appeared after 3 d

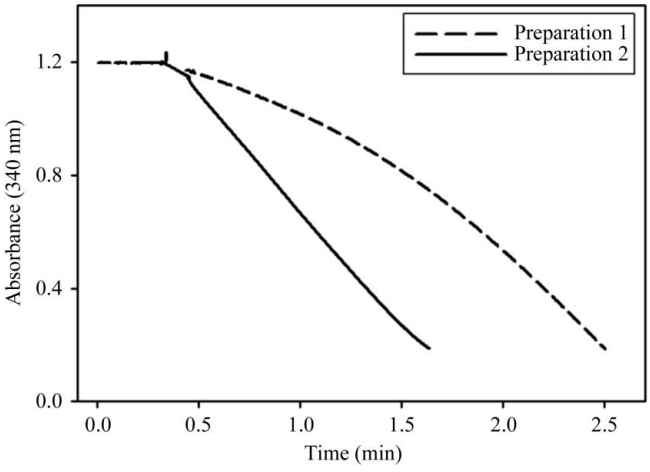

Figure 2
Primary kinetic data comparing *Ba*-DHDPS purified in the absence (preparation 1) and presence (preparation 2) of pyruvate. The reaction was initiated at 0.4 min.

Table 2
X-ray data-collection statistics.

Wavelength (Å)	0.9536439
No. of images	720
Oscillation (°)	0.5
Space group	$P2_12_12_1$
Unit-cell parameters (Å, °)	a = 84.5, b = 124.6, c = 131.0, β = 90.0
Resolution (Å)	37.27–2.15 (2.27–2.15)
Observed reflections	1086285
Unique reflections	75883
Completeness (%)	100 (100)
$R_{\rm merge}$†	0.086 (0.270)
$R_{\rm r.i.m.}$‡	0.089 (0.281)
$R_{\rm p.i.m.}$§	0.023 (0.076)
Mean $I/\sigma(I)$	27.7 (10.0)
Redundancy	14.3 (13.4)
Wilson B value (Å^2)	21.4
Molecules per ASU	4
$V_{\rm M}$ (Å^3 Da^{-1})	2.76
Solvent content (%)	55.5

† $R_{\rm merge} = \sum_{hkl}\sum_i |I_i(hkl) - \langle I(hkl)\rangle| / \sum_{hkl}\sum_i I_i(hkl)$. ‡ $R_{\rm p.i.m.} = \sum_{hkl}[1/(N-1)]^{1/2} \sum_i |I_i(hkl) - \langle I(hkl)\rangle| / \sum_{hkl}\sum_i I_i(hkl)$. § $R_{\rm r.i.m.} = \sum_{hkl}[N/(N-1)]^{1/2}\sum_i |I_i(hkl) - \langle I(hkl)\rangle| / \sum_{hkl}\sum_i I_i(hkl)$.

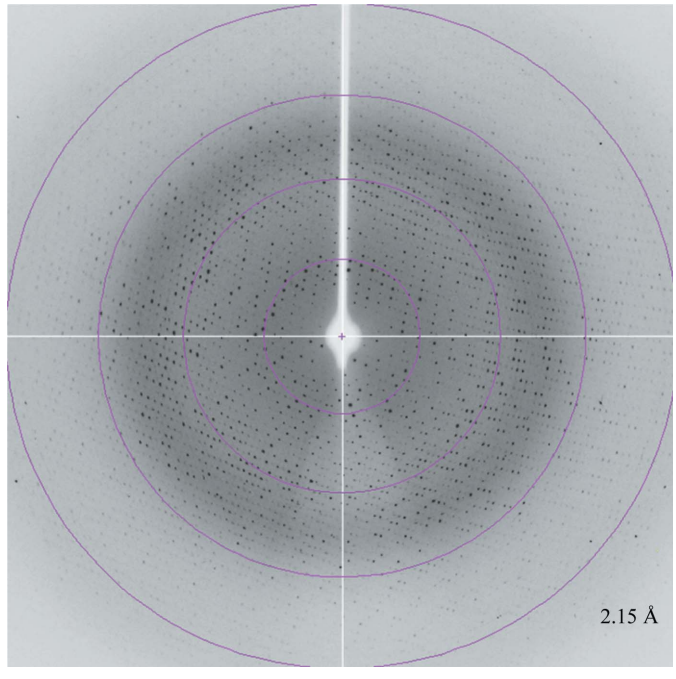

Figure 3
X-ray diffraction pattern from the *Ba*-DHDPS crystal soaked with pyruvate. 2.15 Å refers to the highest resolution spots observed in the outer circle.

and continued to grow to 50 µm in the longest dimension over a further 10 d. Diffraction data were collected from several crystals after soaking with pyruvate, which produced data with a resolution ranging between 2.15 and 2.60 Å. The highest resolution (2.15 Å) data are shown in Fig. 3 and were scaled and merged for analysis.

Similar to the previously reported ligand-free *Ba*-DHDPS structure (Blagova *et al.*, 2006), the space group was determined to be $P2_12_12_1$, with almost identical unit-cell parameters $a = 84.5$, $b = 124.6$, $c = 131.0$ Å. The Matthews coefficient (V_M) was calculated to be 2.8 Å^3 Da^{-1}, with an estimated solvent content of 54%. Scaling and merging of the crystallographic data resulted in an overall R_{merge} of 0.086, with an R_{merge} in the highest resolution shell of 0.27. Complete data-collection statistics are given in Table 2.

Molecular replacement using the program *Phaser* (McCoy, 2007) with the pyruvate-unbound DHDPS from *B. anthracis* as a search model (PDB code 1xky) showed the presence of four monomers in the asymmetric unit. The first round of refinement gave an R_{free} of 23.2% and an R factor of 25.5% and close inspection of the active site showed the presence of electron density consistent with pyruvate bound to Lys163. Further model building and refinement is currently under way. We anticipate that this structure will provide insight into the improved yield and specific activity of the enzyme following purification of *Ba*-DHDPS in the presence of the substrate (Table 1) and the enhanced enzyme-kinetic activity reported in Fig. 2.

We would firstly like to acknowledge the support and assistance of the friendly staff at the Bio21 Collaborative Crystallographic Centre at CSIRO Molecular and Health Technologies, Parkville, Melbourne. We would also like to thank all members of the Perugini laboratory for helpful discussions during the preparation of this manuscript. Finally, we acknowledge the Defense Threat Reduction Agency (DTRA; DTRA Project ID AB07CBT004) and the Australian Research Council for providing an Australian Postdoctoral Fellowship for MAP and a Federation Fellowship for MWP.

References

Blagova, E., Levdikov, V., Milioti, N., Fogg, M. J., Kalliomaa, A. K., Brannigan, J. A., Wilson, K. S. & Wilkinson, A. J. (2006). *Proteins*, **62**, 297–301.
Blickling, S., Renner, C., Laber, B., Pohlenz, H. D., Holak, T. A. & Huber, R. (1997). *Biochemistry*, **36**, 24–33.
Burgess, B. R., Dobson, R. C. J., Bailey, M. F., Atkinson, S. C., Griffin, M. D. W., Jameson, G. B., Parker, M. W., Gerrard, J. A. & Perugini, M. A. (2008). *J. Biol. Chem.* **283**, 27598–27603.
Collaborative Computational Project, Number 4 (1994). *Acta Cryst.* D**50**, 760–763.
Coulter, C. V., Gerrard, J. A., Kraunsoe, J. A. & Pratt, A. J. (1999). *Pestic. Sci.* **55**, 887–895.
Cremer, J., Treptow, C., Eggeling, L. & Sahm, H. (1988). *J. Gen. Microbiol.* **134**, 3221–3229.
Dereppe, C., Bold, G., Ghisalba, O., Ebert, E. & Schar, H. P. (1992). *Plant Physiol.* **98**, 813–821.
Devenish, S. R. A., Gerrard, J. A., Jameson, G. B. & Dobson, R. C. J. (2008). *Acta Cryst.* F**64**, 1092–1095.
Dobson, R. C. J., Griffin, M. D. W., Jameson, G. B. & Gerrard, J. A. (2005). *Acta Cryst.* D**61**, 1116–1124.
Dobson, R. C., Griffin, M. D., Roberts, S. J. & Gerrard, J. A. (2004). *Biochimie*, **86**, 311–315.
Evans, G. & Pettifer, R. F. (2001). *J. Appl. Cryst.* **34**, 82–86.
Frisch, D. A., Gengenbach, B. G., Tommey, A. M., Sellner, J. M., Somers, D. A. & Myers, D. E. (1991). *Plant Physiol.* **96**, 444–452.
Girish, T. S., Sharma, E. & Gopal, B. (2008). *FEBS Lett.* **582**, 2923–2930.
Hutton, C. A., Perugini, M. A. & Gerrard, J. A. (2007). *Mol. Biosyst.* **3**, 458–465.
Kefala, G., Evans, G. L., Griffin, M. D., Devenish, S. R., Pearce, F. G., Perugini, M. A., Gerrard, J. A., Weiss, M. S. & Dobson, R. C. (2008). *Biochem. J.* **411**, 351–360.
Laber, B., Gomis-Ruth, F. X., Romao, M. J. & Huber, R. (1992). *Biochem. J.* **288**, 691–695.
Leslie, A. G. W. (1991). *Crystallographic Computing 5: From Chemistry to Biology*, edited by D. Moras, A. D. Podjarny & J. C. Thierry, pp. 50–61. Oxford University Press.
McCoy, A. J. (2007). *Acta Cryst.* D**63**, 32–41.
McPhillips, T. M., McPhillips, S. E., Chiu, H.-J., Cohen, A. E., Deacon, A. M., Ellis, P. J., Garman, E., Gonzalez, A., Sauter, N. K., Phizackerley, R. P., Soltis, S. M. & Kuhn, P. (2002). *J. Synchrotron Rad.* **9**, 401–406.
Pearce, F. G., Perugini, M. A., McKerchar, H. J. & Gerrard, J. A. (2006). *Biochem. J.* **400**, 359–366.
Wolterink-van Loo, S., Levisson, M., Cabrieres, M. C., Franssen, M. C. & van der Oost, J. (2008). *Extremophiles*, **12**, 461–469.